Magn. Reson., 7, 81–88, 2026
https://doi.org/10.5194/mr-7-81-2026

Open Access
MAGNETIC RESONANCE

Excitation of delocalized long-lived states of aliphatic protons at low and high magnetic fields

Sebastiaan Van Dyck, Coline Wiame, Kirill F. Sheberstov, and Geoffrey Bodenhausen

Chimie Physique et Chimie du Vivant (CPCV, UMR 8228), Département de Chimie, École Normale Supérieure, PSL University, Sorbonne Université, 75005 Paris, France

Correspondence: Kirill F. Sheberstov (kirill.sheberstov@ens.psl.eu)

Received: 19 February 2026 – Discussion started: 9 March 2026
Revised: 21 April 2026 – Accepted: 23 April 2026 – Published: 22 June 2026

Abstract. Long-lived states (LLSs) can be excited in geminal protons of aliphatic chains by mono- or poly-chromatic spin-lock-induced crossings (SLICs), i.e., by application of one or more selective radio frequency (RF) fields, to create delocalized population imbalances between states belonging to different symmetry under spin permutations. At low fields (in this work at 1.4 T or 60 MHz for proton NMR), these experiments are challenging due to the proximity of the chemical shifts and the need to consider the full untruncated J-coupling Hamiltonian. Five molecules were studied in this work: ethanolamine, lysine, vitamin B1, metronidazole, and phenoxyethylamine (POEA). For POEA and metronidazole, the LLSs are reported for the first time. Measurements were carried out at low and high magnetic fields (1.4 and 11.7 T or 60 and 500 MHz for protons) using 60 MHz Magritek and 500 MHz Bruker NEO spectrometers. The rates $R_{\mathrm{LLS}} = 1/T_{\mathrm{LLS}}$ and $R_1 = 1/T_1$ were determined using monochromatic SLIC excitation at both fields. We describe strategies for optimizing SLIC conditions in cases where the signals of neighboring CH_2 groups are relatively close to each other.

1 Introduction

A long-lived state (LLS) is a nuclear spin state that has a lifetime longer than the longitudinal relaxation time (Carravetta and Levitt, 2004). Usually, an LLS corresponds to an imbalance between states with different spin permutation symmetries (Stevanato et al., 2015; Sheberstov et al., 2019; Sabba et al., 2022). In an isolated two-spin system with two protons H_A and $H_{A'}$, such an imbalance can occur between the average population of three symmetric triplet states ($|T_1\rangle$, $|T_0\rangle$, $|T_{-1}\rangle$) and the population of the singlet state ($|S_0\rangle$), which is antisymmetric under spin permutation. The resulting population imbalance is immune to relaxation due to the dipole–dipole coupling between the two protons H_A and $H_{A'}$, thus resulting in a long-lived state. In short *achiral* aliphatic chains – (CH_2–CH_2) – with four protons, the geminal proton pairs are chemically equivalent because of the lack of stereogenic centers, but they can be magnetically inequivalent provided each CH_2 group has a distinct chemical shift and provided the vicinal scalar couplings between neighboring CH_2 groups differ. This occurs if the populations of the rotamers that result from rotations about the C–C bond are *not* equal so that the differences between the vicinal couplings $\Delta J = J_{AX} - J_{AX'} = J_{A'X} - J_{A'X'}$ do not vanish. Magnetic inequivalence allows one to excite an LLS that is *delocalized* across the two AA' and XX' spin pairs. This can be achieved by mono- or poly-chromatic spin-lock-induced crossings (SLICs) (DeVience et al., 2013; Sonnefeld et al., 2022a, b), i.e., by application of one or two selective radio frequency (RF) fields simultaneously. Although long-lived state excitation can, alternatively, also be achieved via adiabatic-passage spin order conversion (APSOC, Pravdivtsev et al., 2016), this work focuses exclusively on mono-chromatic SLIC excitation. At high fields (e.g., 500 MHz), the RF amplitude for single-quantum (SQ) conditions must be $\nu_{\mathrm{SLIC}}^{\mathrm{SQ}} = 2J_{\mathrm{intra}}$, where J_{intra} is an averaged value of the intrapair couplings between geminal protons, e.g., $J_{\mathrm{intra}} = \frac{1}{2}\left\{^2J(H_A, H_{A'}) + ^2J(H_X, H_{X'})\right\}$. A pulse duration $\tau_{\mathrm{SLIC}}^{\mathrm{SQ}} = 1/(|\sqrt{2}\Delta J|)$ allows one to achieve SQ level anti-crossing (LAC). After a variable relaxation delay τ_{rel}, one applies a T_{00} filter which removes all terms other than

the desired population imbalance (Tayler, 2020). A second SLIC pulse then reconverts the LLS into observable magnetization (Fig. 1).

Achiral aliphatic chains with suitable four-spin systems are found in ethanolamine, lysine, vitamin B1, metronidazole, and phenoxyethylamine (POEA) (Fig. 2). At high field (e.g., at 11.7 T or 500 MHz for protons), all aliphatic chains in Fig. 2 can be described as $AA'XX'$ systems in Pople's notation. On the other hand, at low field (e.g., at 1.4 T or 60 MHz), these systems must be described by $AA'BB'$ to account for the second-order couplings. We show that LLS in these molecules can be excited efficiently at 1.4 T despite the strong coupling regime, provided one re-optimizes the SLIC sequences.

2 Methods

2.1 Strong coupling at low field

As previously reported (Sonnefeld et al., 2022a, b), the Hamiltonian of a four-spin $AA'XX'$ system at high magnetic fields (in this work, at 11.7 T) only features strong couplings between the geminal pairs (e.g., H_A couples strongly to $H_{A'}$) but not between the vicinal protons (H_A couples weakly to H_X). Strong coupling is defined by $\Delta\delta < J$, whereas weak coupling holds when $\Delta\delta \gg J$. For a four-spin system, $\Delta\delta$ is defined by the difference in chemical shift between the two adjacent CH_2 spin pairs AA' and XX'.

The J couplings are constant. However, $\Delta\delta$ scales with the magnetic field; therefore, as we move to a lower magnetic field, $\Delta\delta$ decreases, which results in a higher ratio of J with respect to $\Delta\delta$. Therefore, the couplings between geminal proton spin pairs become stronger. That is why the Hamiltonian at low magnetic field (i.e., 1.4 T) may be represented by the topological diagram shown in Fig. 3, where the geminal couplings $J_{AA'}$ and $J_{BB'}$ are approximately equal, while the vicinal couplings are pairwise degenerate $J_{AB} = J_{A'B'}$ and $J_{A'B} = J_{AB'}$.

The Hamiltonian in units of Hz is

$$\begin{aligned} H = {} & \nu_{AA'}\left(\hat{\boldsymbol{I}}_{Az} + \hat{\boldsymbol{I}}_{Az'}\right) + \nu_{BB'}\left(\hat{\boldsymbol{I}}_{Bz} + \hat{\boldsymbol{I}}_{Bz'}\right) \\ & + J_{AA'}\hat{\boldsymbol{I}}_A \cdot \hat{\boldsymbol{I}}_{A'} + J_{BB'}\hat{\boldsymbol{I}}_B \cdot \hat{\boldsymbol{I}}_{B'} + J_{AB}\hat{\boldsymbol{I}}_A \cdot \hat{\boldsymbol{I}}_B \\ & + J_{AB'}\hat{\boldsymbol{I}}_A \cdot \hat{\boldsymbol{I}}_{B'} + J_{A'B}\hat{\boldsymbol{I}}_{A'} \cdot \hat{\boldsymbol{I}}_B + J_{A'B'}\hat{\boldsymbol{I}}_{A'} \cdot \hat{\boldsymbol{I}}_{B'} \end{aligned} \quad (1)$$

where $\hat{I}_i$ corresponds to the vector representation of the spin operator of spin i, and the operator $\hat{I}_{iz}$ represents the z component of the operator $\hat{I}_i$. When switching from strong coupling at low field to weak coupling at high field, the non-secular terms of the vicinal J couplings (but not those due to the geminal couplings) can be dropped.

$$\begin{aligned} H_{\text{vic}}^{\text{LF}} = {} & J_{AB}\hat{\boldsymbol{I}}_A \cdot \hat{\boldsymbol{I}}_B + J_{AB'}\hat{\boldsymbol{I}}_A \cdot \hat{\boldsymbol{I}}_{B'} + J_{A'B}\hat{\boldsymbol{I}}_{A'} \cdot \hat{\boldsymbol{I}}_B \\ & + J_{A'B'}\hat{\boldsymbol{I}}_{A'} \cdot \hat{\boldsymbol{I}}_{B'} \\ H_{\text{vic}}^{\text{HF}} = {} & J_{AB}\hat{\boldsymbol{I}}_{Az}\hat{\boldsymbol{I}}_{Bz} + J_{AB'}\hat{\boldsymbol{I}}_{Az}\hat{\boldsymbol{I}}_{Bz'} \\ & + J_{A'B}\hat{\boldsymbol{I}}_{Az'}\hat{\boldsymbol{I}}_{Bz} + J_{A'B'}\hat{\boldsymbol{I}}_{Az'}\hat{\boldsymbol{I}}_{Bz'} \end{aligned} \quad (2)$$

2.2 Effects of second-order vicinal couplings

In a low static field, a weak RF field applied to H_A and $H_{A'}$ also affects the protons H_B and $H_{B'}$. At high field, these effects are negligible so that monochromatic SLIC is truly selective. At low magnetic fields, we have investigated the effects of second-order couplings for mono-chromatic SLIC excitation using simulations with Spin Dynamica (Bengs and Levitt, 2018), written using the Wolfram Mathematica software package.

In a four-spin system $AA'BB'$, the LLS part of the density operator $\hat{\sigma}_{\text{LLS}}$, i.e., the population imbalances, always comprises three terms, regardless of how one excites the LLS (Sonnefeld et al., 2022b):

$$\begin{aligned} \hat{\sigma}_{\text{LLS}} = {} & \lambda_{\text{LLS}}\Bigg(-\frac{1}{3}\hat{\boldsymbol{I}}_A \cdot \hat{\boldsymbol{I}}_{A'} - \frac{1}{3}\hat{\boldsymbol{I}}_B \cdot \hat{\boldsymbol{I}}_{B'} + \frac{8}{9}\left(\hat{\boldsymbol{I}}_A \cdot \hat{\boldsymbol{I}}_{A'}\right) \\ & \cdot \left(\hat{\boldsymbol{I}}_B \cdot \hat{\boldsymbol{I}}_{B'}\right)\Bigg). \end{aligned} \quad (3)$$

The LLS yields have been simulated for mono-chromatic SLIC irradiation applied to AA'. We chose typical values for a four-spin system: $J_{AA'} = J_{BB'} = -14$ Hz, $J_{AB} = J_{A'B'} = 5$ Hz and $J_{A'B} = J_{AB'} = 9$ Hz; hence, $\Delta J = -4$ Hz. At high fields, where the secular approximation can be invoked, the optimum RF amplitude for the single-quantum (SQ-LAC) condition is $\nu_{\text{SLIC}} = |2J_{\text{intra}}| = 28$ Hz, and the optimum SLIC duration is $\tau_{\text{SLIC}} = 1/(\Delta J\sqrt{2}) = 177$ ms (Sonnefeld et al., 2022a).

Figure 4 also shows how the LLS yield depends on the chemical shift difference between spins pairs AA' and BB'. The simulations were done for high-field SLIC conditions ($\nu_{\text{SLIC}} = 28$ Hz, $\tau_{\text{SLIC}} = 177$ ms). At $\Delta\delta > 60$ Hz the LLS yield reaches a plateau that was normalized to 1. The sudden drop in LLS yield – here, at 50 Hz – depends on J_{intra}; for higher values of J_{intra}, the dip shifts to higher frequencies. This means there is a "blind spot" where excitation of LLS cannot be achieved, at least not starting with high-field SLIC parameters. The blind spot can be understood from the dynamics of the off-resonant BB' spins in the rotating frame. Although these spins are not meant to be directly addressed by the SLIC irradiation applied to the AA' pair, they experience an effective field of magnitude $\nu_1^{\text{eff}} = \sqrt{\Delta\delta^2 + \nu_{\text{SLIC}}^2}$, where $\Delta\delta$ is the frequency offset between the two spin pairs. The dip in the LLS efficiency occurs when this effective nutation frequency matches $2\nu_{\text{SLIC}}$, which gives the condition $\Delta\delta = \sqrt{3}\nu_{\text{SLIC}}$.

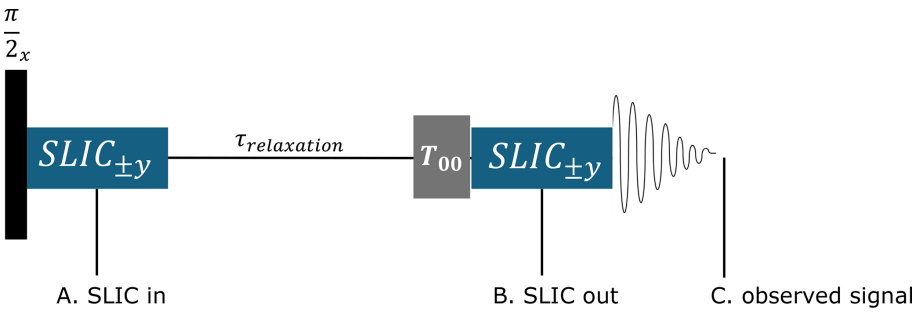

Figure 1. Sequence for the measurement of the relaxation times T_{LLS} of long-lived states (LLSs) of protons in aliphatic chains comprising $AA'XX'$ or $AA'BB'$ systems. The $\pi/2$ pulse brings the magnetization into the transverse plane. The first spin-lock-induced-crossing (SLIC) pulse converts this magnetization into an LLS. This pulse is followed by a variable delay and a T_{00} filter that retains only singlet order, while the second SLIC pulse reconverts the LLS into observable magnetization. Cycling of the RF phases along the $\pm y$ axes eliminates undesirable signals (Kiryutin et al., 2016). In $AA'XX'$ or $AA'BB'$ systems, the SLIC pulses must be applied on resonance with AA', BB', or XX' spins.

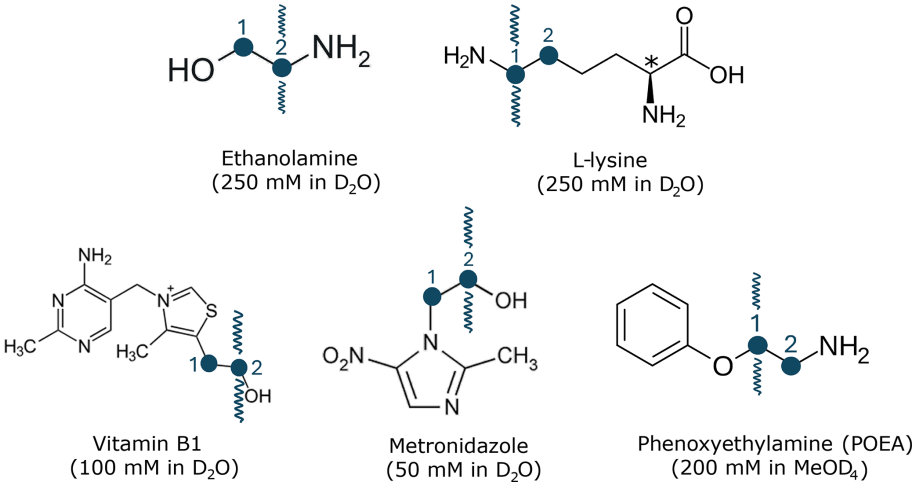

Figure 2. Five molecules where long-lived states have been excited efficiently at both low and high static fields of 1.4 and 11.7 T (60 and 500 MHz for protons). All molecules feature chemically equivalent but *magnetically inequivalent* proton pairs of $AA'XX'$ at high field and $AA'BB'$ at low field. The wavy arrows indicate the CH_2 groups that were irradiated in these experiments to excite the LLS by monochromatic SLIC (arrows above the molecules) and to reconvert the LLS into magnetization (arrows below the molecules). Note that one can also reconvert LLS on the adjacent CH_2 group. The relaxation rates $R_1 = 1/T_1$ of the CH_2 groups were determined by the conventional inversion–recovery method. All ligands were dissolved in D_2O at concentrations in the range between 50 and 250 mM, except for POEA, which was dissolved in $MeOD_4$. The samples were not buffered. The pH values are 11.70 for ethanolamine, 6.00 for L-lysine, 2.70 for vitamin B1, 7.15 for metronidazole, and 10.65 for POEA.

In Fig. 4, under high-field SLIC conditions ($\nu_{\mathrm{SLIC}} = 28$ Hz, $\tau_{\mathrm{SLIC}} = 177$ ms), the LLS yield is 1.0 for 250 Hz and drops down to 0.35 for $\Delta\delta = 52$ Hz. Figure 4 shows how the LLS yield depends on the chemical shift difference.

The simulations of Fig. 5 show how to optimize the RF amplitude ν_{SLIC} and the SLIC duration τ_{SLIC}, for the strong coupling regime and single-quantum conditions, to achieve the best LLS yields at different values for $\Delta\delta = 250$ Hz (high-field regime) and $\Delta\delta = 52$ Hz (low-field regime). The figure shows the LLS conversion efficiency normalized to 1 with respect to the high-field regime, which is achieved at the plateau on the right-hand side of the figure. The maximum conversion efficiency in aliphatic spin networks for 4 spin systems for monochromatic SLIC applied to AA' spins is achieved when a full population of the $T_{+1}^{AA'}T_0^{BB'}$ or $T_{-1}^{AA'}T_0^{BB'}$ state is transferred to the $S_0^{AA'}S_0^{BB'}$ state. This corresponds to ca. $5/72 \approx 7\,\%$ population imbalance between the 9 triplet-triplet states and the unique singlet-singlet state.

According to Fig. 5, the LLS yield after re-optimization of ν_{SLIC} and τ_{SLIC} is 0.8 for $\Delta\delta = 52$ Hz. We can compare it with the LLS yield in Fig. 4 (~ 0.35) to obtain the enhancement factor. The ratio of the optimized LLS yield to the non-optimized LLS yield is $0.8/0.35 \approx 2.3$.

Subsequently, we re-optimized τ_{SLIC} and ν_{SLIC} for each molecule experimentally. The SLIC conditions at 11.7 and

Table 1. Experimentally optimized SLIC conditions for four-spin systems at low (1.4 T) and high (11.7 T) fields. The SLIC amplitude υ_{SLIC} changes for vitamin B1 and metronidazole but remains unchanged for the other ligands. The duration τ_{SLIC} increases at a low magnetic field for ethanolamine, vitamin B1, and metronidazole. Note that the reported SLIC conditions for ethanolamine and vitamin B1 deviate from previously reported values (Sonnefeld et al., 2022b) as the molecules in this work were not prepared in buffer. Shifts in pH values can affect SLIC conditions, particularly for ethanolamine. The reported pH values for molecules prepared in D_2O are as follows: 11.70 for ethanolamine, 6.00 for lysine, 2.70 for vitamin B1, and 7.15 for metronidazole.

Molecule	$\Delta\delta$ (Hz) at 1.4 T (60 MHz)	υ_{SLIC} (Hz) at 11.7 T (500 MHz)	υ_{SLIC} (Hz) at 1.4 T (60 MHz)	τ_{SLIC} (ms) at 11.7 T (500 MHz)	τ_{SLIC} (ms) at 1.4 T (60 MHz)
Ethanolamine	54	24	25	350	380
Lysine	80	27	27	205	205
Vitamin B1	42	26	27	240	320
Metronidazole	36	26	27	250	310
POEA	61	23	23	240	240

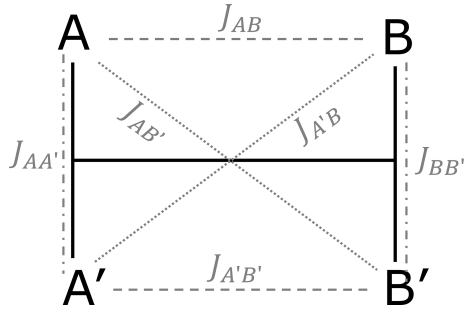

Figure 3. Topological representation of a four-spin $AA'BB'$ system.

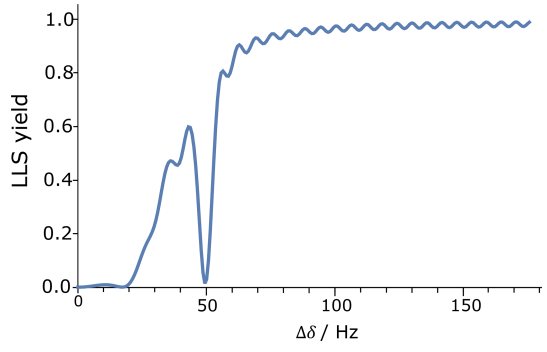

Figure 4. Simulated yields of the excitation of a long-lived state (LLS) as defined in Eq. (3) as a function of the chemical shift difference ($\Delta\delta$) between the AA' and BB' spin pairs in a four-spin system. Parameters of the SLIC pulse were $\upsilon_{SLIC} = 28$ Hz and $\tau_{SLIC} = 177$ ms, corresponding to the high-field SLIC conditions. The LLS yield is normalized to 1 with respect to the high-field regime, which is achieved at the plateau on the right-hand side of the figure.

1.4 T are displayed in Table 1, whereas Table 2 shows the improvement in the experimentally achieved LLS yield upon re-optimization of τ_{SLIC} and υ_{SLIC} at 1.4 T.

3 Comparing T_{LLS} and T_1 relaxation time constants at different magnetic fields

The T_1 and T_{LLS} of all five molecules shown in Fig. 2 were measured at low and high static fields, in the same sample tubes, at the same concentrations, in the same solvents, and at the same temperatures. The concentrations were chosen to be high to warrant sufficient sensitivity at low field, bearing in mind that the efficiency of two-way ("in-and-out") SLIC is on the order of only 10 %. In the future we aim to enhance the sensitivity by combining SLIC at both low and high fields with dynamic nuclear polarization (Vasos et al., 2009; Tayler et al., 2012; Bornet et al., 2014; Kiryutin et al., 2019a, b; Razanahoera et al., 2024).

The ratios of the relaxation rates of long-lived states ($R_{LLS} = 1/T_{LLS}$) and of longitudinal magnetization ($R_1 = 1/T_1$), are different at low and high fields (60 and 500 MHz for protons). The ratio T_{LLS}/T_1 provides a measure of the usefulness of LLS for various applications such as the measurement of slow motions (Sarkar et al., 2007) or small translational diffusion coefficients (Cavadini et al., 2005).

4 Results and discussion

Inversion–recovery experiments at both low and high fields provided T_1 values for all samples. The signal integrals of a chosen multiplet (see wavy arrows in Fig. 2) were plotted as a function of the relaxation delay τ_{rel}. Figures 6 and 7 show the results obtained at low field. The same T_1 experiments were repeated at high magnetic field (11.7 T). The results are summarized in Table 3.

To determine the lifetimes T_{LLS} at low field (1.4 T) by means of SLIC experiments, the delay τ_{rel} in Fig. 1 was incremented for each of the five molecules shown in Fig. 2.

Again, these experiments were also carried out with the same samples at high field. The high- and low-field results are shown in Tables 3 and 4. The effect of the magnetic field on the ratio T_{LLS}/T_1 is shown in Table 5.

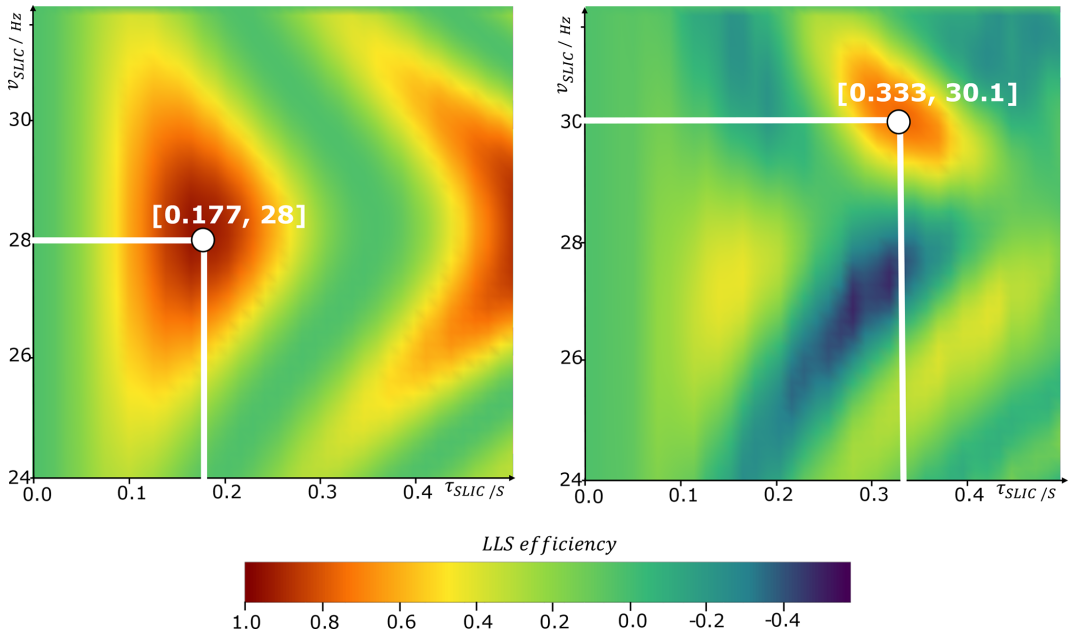

Figure 5. Left panel shows that, for a large difference $\Delta\delta = 250$ Hz, the single-quantum SLIC condition (RF amplitude ν_{SLIC} in the vertical dimension and the duration τ_{SLIC} in the horizontal dimension) for a four-spin system ($\nu_{SLIC} = 28$ Hz, $\tau_{SLIC} = 177$ ms) match the theoretical conditions at high field ($\nu_{SLIC} = |2J_{intra}|$, $\tau_{SLIC} = 1/(\Delta J\sqrt{2})$). However, when the difference is small ($\Delta\delta = 52$ Hz), the optimum SLIC conditions are $\nu_{SLIC} = 30.1$ Hz, while $\tau_{SLIC} = 333$ ms. The change in ν_{SLIC} is subtle (+7 %), but the SLIC duration changes drastically (+83 %). Since aliphatic – CH_2 – groups in many of the selected molecules (Fig. 2) have $\Delta\delta < 60$ Hz at 1.4 T, their SLIC duration τ_{SLIC} and SLIC amplitude ν_{SLIC} must be re-optimized. The LLS efficiency is normalized to 1 with respect to the high-field regime, which is achieved at the maximum on the left panel.

Table 2. LLS yield at 1.4 T before re-optimization of ν_{SLIC} and τ_{SLIC} (using the conditions listed in columns 3 and 5 in Table 1) and after re-optimization of ν_{SLIC} and τ_{SLIC} (using the conditions listed in column 4 and 6 in Table 1). The LLS yield with respect to the thermal signal (when the number of transients and the receiver gain remain the same) is lower than at conventional high field, where the yield is approximately ~ 10 % (Sonnefeld et al., 2022b). However, the third column shows that an enhancement, up to a factor of 3.6, has been achieved. This illustrates the need for re-optimization of ν_{SLIC} and τ_{SLIC} when $\Delta\delta < 60$ Hz at low magnetic fields. For lysine and POEA, for which the difference in chemical shifts $\Delta\delta > 60$ Hz, the SLIC conditions were identical at 11.7 and 1.4 T, and so no increase in yield was observed.

Molecule	LLS yield (with respect to thermal) (non-optimized SLIC)/%	LLS yield (with respect to thermal) (optimized SLIC)/%	Enhancement factor (optimized/ non-optimized)
Ethanolamine	5.68	6.25	1.1
Lysine	2.55	2.55	1.0
Vitamin B1	2.12	3.50	1.7
Metronidazole	1.11	4.06	3.6
POEA	6.25	6.25	1.0

Comparison between the relaxation times T_{LLS} and T_1 at high field gives a range $3.0 < T_{LLS}/T_1 < 4.2$ for all molecules except vitamin B1, which has an exceptional gain $T_{LLS}/T_1 = 7.6$. At low field, by contrast, the ratios lie in the range of $3.0 < T_{LLS}/T_1 < 6.8$ for all molecules except lysine, which has a rather modest gain $T_{LLS}/T_1 = 1.6$. In summary, the T_{LLS}/T_1 ratios at high field (11.7 T) are either slightly higher or similar compared to those at low field (1.4 T), except for ethanolamine, where the enhancement is 17 % higher at low field.

5 Conclusions

The yield of the excitation of LLS by SLIC at low fields depends on the chemical shift difference $\Delta\delta$ between the neighboring spin pairs. When $\Delta\delta \leq 60$ Hz, the pulse amplitude, ν_{SLIC}, and duration, τ_{SLIC}, must be optimized experimen-

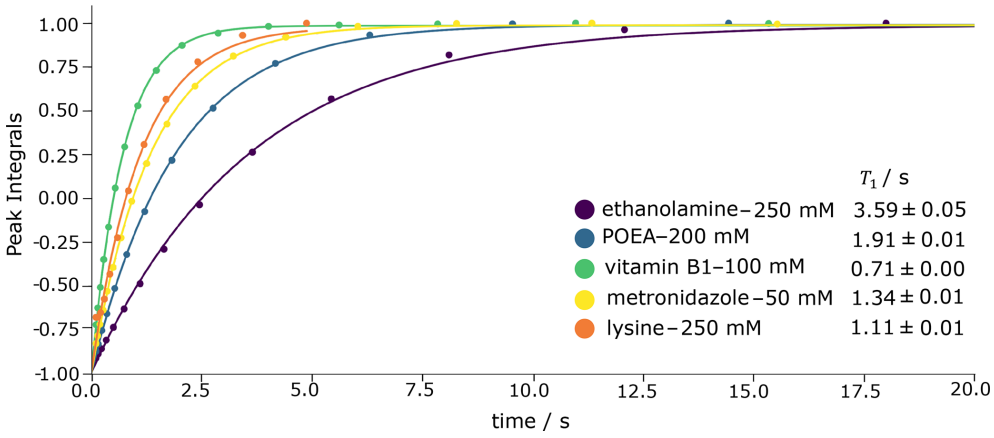

Figure 6. Longitudinal T_1 relaxation at low field (1.4 T) of the CH_2 protons highlighted by dots in the five molecules shown in Fig. 2, measured by inversion recovery.

Table 3. T_1 and T_{LLS} values at high field (11.7 T).

Molecule	(mM)	CH_2 group (see Fig. 2)	T_1^{HF} (s) (500 MHz)	T_{LLS}^{HF} (s) (500 MHz)
Ethanolamine	250	2	3.46 ± 0.01	10.33 ± 1.88
Lysine	250	1	1.40 ± 0.01	4.33 ± 0.08
Vitamin B1	100	2	0.73 ± 0.01	5.58 ± 0.27
Metronidazole	50	2	1.27 ± 0.02	3.81 ± 0.14
POEA	200	1	2.21 ± 0.02	9.21 ± 0.49

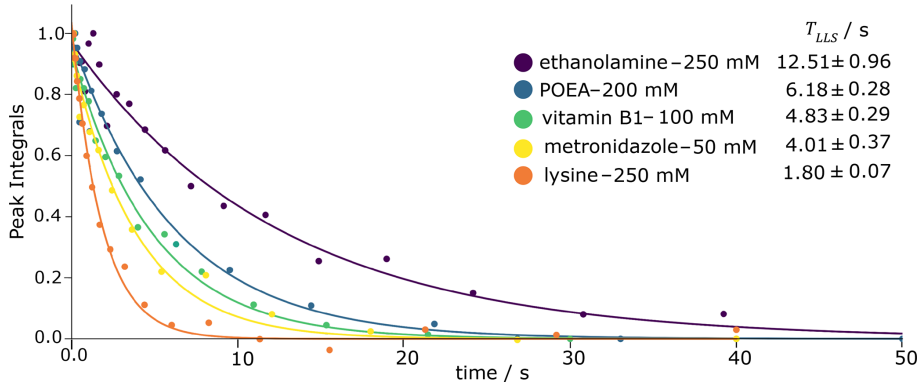

Figure 7. LLS decays at low field (1.4 T) of the aliphatic CH_2 protons highlighted by curly arrows in the five molecules drawn Fig. 2.

Table 4. T_1 and T_{LLS} values at low field (1.4 T or 60 MHz for protons).

Molecule	(mM)	CH_2 group (see Fig. 2)	T_1^{LF} LF (s) (60 MHz)	T_{LLS}^{LF} (s) (60 MHz)
Ethanolamine	250	2	3.59 ± 0.05	12.51 ± 0.96
Lysine	250	1	1.11 ± 0.01	1.80 ± 0.07
Vitamin B1	100	2	0.71 ± 0.00	4.83 ± 0.29
Metronidazole	50	2	1.34 ± 0.01	4.01 ± 0.37
POEA	200	1	1.91 ± 0.01	6.18 ± 0.28

Table 5. Ratios T_{LLS}/T_1 at high field (11.7 T) and at low field (1.4 T).

Molecule in D_2O	(mM)	Enhancement $(T_{LLS}/T_1)^{HF}$ (500 MHz)	Enhancement $(T_{LLS}/T_1)^{LF}$ (60 MHz)	Ratio of enhancements HF / LF
Ethanolamine	250	3.0	3.5	0.86
Lysine	250	3.1	1.6	1.94
Vitamin B1	100	7.6	6.8	1.12
Metronidazole	50	3.0	3.0	1.00
POEA	200	4.2	3.2	1.31

tally, starting at the high-field conditions. The T_{LLS}/T_1 ratios at low field (1.4 T) are either slightly lower or similar as at high field.

Code availability. The Spin Dynamica codes used to calculate Figs. 4 and 5 are available through the Zenodo repository under https://doi.org/10.5281/zenodo.18684154 (Sheberstov, 2026b).

Data availability. The data with inversion recovery and LLS experiments, together with SLIC pulse sequences for Spinsolve Expert, are available at https://doi.org/10.5281/zenodo.20597567 (Sheberstov, 2026a).

Author contributions. KFS designed the research. SVD and CW performed the experiments and analyzed the data. All of the authors contributed to writing the paper.

Competing interests. At least one of the (co-)authors is a member of the editorial board of *Magnetic Resonance*. The peer-review process was guided by an independent editor, and the authors also have no other competing interests to declare.

Disclaimer. Publisher's note: Copernicus Publications remains neutral with regard to jurisdictional claims made in the text, published maps, institutional affiliations, or any other geographical representation in this paper. The authors bear the ultimate responsibility for providing appropriate place names. Views expressed in the text are those of the authors and do not necessarily reflect the views of the publisher.

Acknowledgements. We are grateful to the reviewers, Danila A. Barskiy and Mohammed Sabba, who helped us improve the quality of the paper.

Financial support. This work was supported by the European Research Council (ERC), Synergy grant "Highly Informative Drug Screening by Overcoming NMR Restrictions" (HISCORE, grant agreement no. 951459). Kirill F. Sheberstov acknowledges support by l'Agence Nationale de la Recherche (ANR) on the project THROUGH-NMR (grant no. ANR-24-CE93-0011-01).

Review statement. This paper was edited by Patrick Giraudeau and reviewed by Danila A. Barskiy and Mohamed Sabba.

References

Bengs, C. and Levitt, M. H.: SpinDynamica: Symbolic and numerical magnetic resonance in a Mathematica environment, Magn. Reson. Chem., 56, 374–414, https://doi.org/10.1002/mrc.4642, 2018.

Bornet, A., Ji, X., Mammoli, D., Vuichoud, B., Milani, J., Bodenhausen, G., and Jannin, S.: Long-Lived States of Magnetically Equivalent Spins Populated by Dissolution-DNP and Revealed by Enzymatic Reactions, Chem.-Eur. J., 20, 17113–17118, https://doi.org/10.1002/chem.201404967, 2014.

Carravetta, M. and Levitt, M. H.: Long-lived nuclear spin states in high-field solution NMR, J. Am. Chem. Soc., 126, 6228–6229, https://doi.org/10.1021/ja0490931, 2004.

Cavadini, S., Dittmer, J., Antonijevic, S., and Bodenhausen, G.: Slow Diffusion by Singlet State NMR Spectroscopy, J. Am. Chem. Soc., 127, 15744–15748, https://doi.org/10.1021/ja052897b, 2005.

DeVience, S. J., Walsworth, R. L., and Rosen, M. S.: Preparation of Nuclear Spin Singlet States Using Spin-Lock Induced Crossing, Phys. Rev. Lett., 111, 173002, https://doi.org/10.1103/PhysRevLett.111.173002, 2013.

Kiryutin, A. S., Pravdivtsev, A. N., Yurkovskaya, A. V., Vieth, H.-M., and Ivanov, K. L.: Nuclear Spin Singlet Order Selection by Adiabatically Ramped RF Fields, J. Phys. Chem. B, 120, 11978–11986, https://doi.org/10.1021/acs.jpcb.6b08879, 2016.

Kiryutin, A. S., Panov, M. S., Yurkovskaya, A. V., Ivanov, K. L., and Bodenhausen, G.: Proton Relaxometry of Long-Lived Spin Order, Chem. Phys. Chem., 20, 766–772, https://doi.org/10.1002/cphc.201800960, 2019a.

Kiryutin, A. S., Rodin, B. A., Yurkovskaya, A. V., Ivanov, K. L., Kurzbach, D., Jannin, S., Guarin, D., Abergel, D., and Bodenhausen, G.: Transport of hyperpolarized samples in dissolution-DNP experiments, Phys. Chem. Chem. Phys., 21, 13696–13705, https://doi.org/10.1039/C9CP02600B, 2019b.

Pravdivtsev, A. N., Kiryutin, A. S., Yurkovskaya, A. V., Vieth, H.-M., and Ivanov, K. L.: Robust conversion of singlet spin order in coupled spin-1/2 pairs by adiabat-

ically ramped RF-fields, J. Magn. Reson., 273, 56–64, https://doi.org/10.1016/j.jmr.2016.10.003, 2016.

Razanahoera, A., Sonnefeld, A., Sheberstov, K., Narwal, P., Minaei, M., Kouřil, K., Bodenhausen, G., and Meier, B.: Hyperpolarization of Long-Lived States of Protons in Aliphatic Chains by Bullet Dynamic Nuclear Polarization, Revealed on the Fly by Spin-Lock-Induced Crossing, J. Phys. Chem. Lett., 15, 9024–9029, https://doi.org/10.1021/acs.jpclett.4c01457, 2024.

Sabba, M., Wili, N., Bengs, C., Whipham, J. W., Brown, L. J., and Levitt, M. H.: Symmetry-based singlet–triplet excitation in solution nuclear magnetic resonance, J. Chem. Phys., 157, 134302, https://doi.org/10.1063/5.0103122, 2022.

Sarkar, R., Vasos, P. R., and Bodenhausen, G.: Singlet-State Exchange NMR Spectroscopy for the Study of Very Slow Dynamic Processes, J. Am. Chem. Soc., 129, 328–334, https://doi.org/10.1021/ja0647396, 2007.

Sheberstov, K.: Experiments and Magritek pulse sequences for the article on "Excitation of Delocalized Long-Lived States in Aliphatic Protons at Low and High Magnetic Fields", Zenodo [data set], https://doi.org/10.5281/zenodo.20597567, 2026a.

Sheberstov, K. F.: Source code for "Excitation of Delocalized Long-Lived States in Aliphatic Protons at Low and High Magnetic Fields", Zenodo [code], https://doi.org/10.5281/zenodo.18684154, 2026b.

Sheberstov, K. F., Kiryutin, A. S., Bengs, C., Hill-Cousins, J. T., Brown, L. J., Brown, R. C. D., Pileio, G., Levitt, M. H., Yurkovskaya, A. V., and Ivanov, K. L.: Excitation of singlet–triplet coherences in pairs of nearly-equivalent spins, Phys. Chem. Chem. Phys., 21, 6087–6100, https://doi.org/10.1039/C9CP00451C, 2019.

Sonnefeld, A., Bodenhausen, G., and Sheberstov, K.: Polychromatic Excitation of Delocalized Long-Lived Proton Spin States in Aliphatic Chains, Phys. Rev. Lett., 129, 183203, https://doi.org/10.1103/PhysRevLett.129.183203, 2022a.

Sonnefeld, A., Razanahoera, A., Pelupessy, P., Bodenhausen, G., and Sheberstov, K.: Long-lived states of methylene protons in achiral molecules, Sci. Adv., 8, eade2113, https://doi.org/10.1126/sciadv.ade2113, 2022b.

Stevanato, G., Hill-Cousins, J. T., Håkansson, P., Roy, S. S., Brown, L. J., Brown, R. C. D., Pileio, G., and Levitt, M. H.: A Nuclear Singlet Lifetime of More than One Hour in Room-Temperature Solution, Angew. Chem. Int. Ed., 54, 3740–3743, https://doi.org/10.1002/anie.201411978, 2015.

Tayler, M. C. D.: Filters for Long-lived Spin Order, The Royal Society of Chemistry, 188–208, https://doi.org/10.1039/9781788019972-00188, 2020.

Tayler, M. C. D., Marco-Rius, I., Kettunen, M. I., Brindle, K. M., Levitt, M. H., and Pileio, G.: Direct Enhancement of Nuclear Singlet Order by Dynamic Nuclear Polarization, J. Am. Chem. Soc., 134, 7668–7671, https://doi.org/10.1021/ja302814e, 2012.

Vasos, P. R., Comment, A., Sarkar, R., Ahuja, P., Jannin, S., Ansermet, J.-P., Konter, J. A., Hautle, P., van den Brandt, B., and Bodenhausen, G.: Long-lived states to sustain hyperpolarized magnetization, P. Natl. Acad. Sci. USA, 106, 18469–18473, https://doi.org/10.1073/pnas.0908123106, 2009.